Menguc, Y.; Yong-Lae Park; Martinez-Villalpando, E.; Aubin, P.; Zisook, M.; Stirling, L.; Wood, R.J.; Walsh, C.J., "Soft wearable motion sensing suit for lower limb biomechanics measurements," *Robotics and Automation (ICRA), 2013 IEEE International Conference on,* pp.5309-5316, 6-10 May 2013

http://ieeexplore.ieee.org/stamp/stamp.jsp?tp=&arnumber=6631337&isnumber=6630547

Soft Wearable Motion Sensing Suit for Lower Limb Biomechanics Measurements*

Yiğit Mengüç[1,2], Yong-Lae Park[1,2], Ernesto Martinez-Villalpando[1,2], Patrick Aubin[1,2], Miriam Zisook[1], Leia Stirling[1], Robert J. Wood[1,2], Conor J. Walsh[1,2,3]

***Abstract*— Motion sensing has played an important role in the study of human biomechanics as well as the entertainment industry. Although existing technologies, such as optical or inertial based motion capture systems, have relatively high accuracy in detecting body motions, they still have inherent limitations with regards to mobility and wearability. In this paper, we present a soft motion sensing suit for measuring lower extremity joint motion. The sensing suit prototype includes a pair of elastic tights and three hyperelastic strain sensors. The strain sensors are made of silicone elastomer with embedded microchannels filled with conductive liquid. To form a sensing suit, these sensors are attached at the hip, knee, and ankle areas to measure the joint angles in the sagittal plane. The prototype motion sensing suit has significant potential as an autonomous system that can be worn by individuals during many activities outside the laboratory, from running to rock climbing. In this study we characterize the hyperelastic sensors in isolation to determine their mechanical and electrical responses to strain, and then demonstrate the sensing capability of the integrated suit in comparison with a ground truth optical motion capture system. Using simple calibration techniques, we can accurately track joint angles and gait phase. Our efforts result in a calculated trade off: with a maximum error less than 8%, the sensing suit does not track joints as accurately as optical motion capture, but its wearability means that it is not constrained to use only in a lab.**

I. Introduction

The field of soft robotics is generating new applications, causing human-robot interaction to become more commonplace and natural. In particular with wearable devices, we are seeing a shift away from traditional exoskeletons that use rigid components to those that use primarily soft materials to apply assistive torques to the wearer's joints [1]. Here we present a soft sensing suit intended to be worn by impaired or healthy individuals with the goal of measuring lower limb joint motion during a variety of activities. We envision the suit will operate as a stand-alone sensing system and eventually provide feedback for a wearable soft exoskeleton suit. The enabling technologies are two-fold: hyperelastic, liquid metal embedded sensors that can detect strains up to 300% and a specially designed garment that interfaces the sensors with the user (Fig. 1).

The entertainment industry uses motion capture to directly measure the motion of the wearer in order to puppet a computer generated avatar. As scientists, we are interested in capturing human motion data in order to understand the underlying biomechanics. Simulation tools such as OpenSim [2] attempt to recreate the musculoskeletal system from data taken with motion capture and muscle activation sensors (electromyography, EMG). By applying motion capture data to musculoskeletal models, it is possible to identify causes for gait pathologies, to determine when athletes become fatigued, and even identify causes for and possibly prevent injury [3]. In recent years the healthcare, sports and consumer industries have seen an increase in the use of other wearable sensing systems for personal monitoring of physiological signals (e.g. heart rate) as well as tracking running or other activities (shoe mounted IMUs) [4].

Traditionally, biomechanical data is gathered using rigid, computationally-intensive and lab-constrained devices such as electronic goniometers, inertial-measurement units, and optical motion capture systems. Each of these systems have their strengths and weaknesses. Adhesives used for attaching the devices to clothing or skin directly can fail during vigorous motions or when the skin becomes sweaty. Inertial-measurement unit (IMU) signals drift and must be corrected

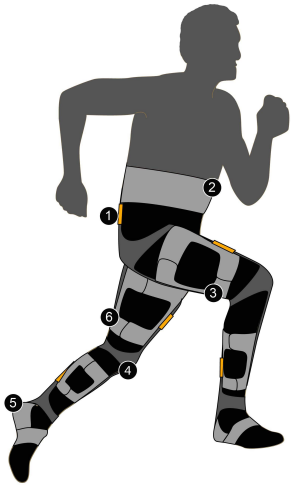

Fig. 1. Illustration of the concept of a soft wearable motion sensing suit for the lower extremities. Key design elements include: (1) a hyperelastic strain sensor is sewn to an inextensible strap, (2) a waist strap secures a sensor above the hip on the dorsal side, (3) a thigh strap secures a sensor below the hip on the back and above the knee on the ventral side, (4) a calf strap secures a sensor below the knee on the ventral side and above the ankle on the dorsal side, (5) a heel stirrup secures a sensor below the ankle on the dorsal side, (6) compliant, flexible membranes cover sensors and straps, with have tabs to secure the sensors around the joints.

* This work was funded by the Wyss Institute for Biologically Inspired Engineering at Harvard University

[1]Wyss Institute for Biologically Inspired Engineering at Harvard University, Boston, MA, 02115, USA.

[2]School of Engineering and Applied Sciences, Harvard University, Cambridge, MA 02138, USA.

[3]email: walsh@seas.harvard.edu

with intensive computational processing or some external signal that helps re-calibrate the sensor [5]. Optical motion capture is considered the gold standard tool for measuring human kinematics from cinema to medicine, but is expensive and inherently limited to a fixed volume. As wearable electromechanical devices become more mature, more emphasis is being placed on using wearable motion capture technology for collecting biomechanical data [6]. The soft-sensor suit prototype that we present has the ability to sense joint angles of the wearer in an unencumbered, tetherless and field-ready form. Also, the suit can be significantly less expensive than alternative motion capture systems.

Our bodies sense position (proprioception) and orientation of the limb segments mechanically, with a combination of absolute muscle stretch and stretch rate sensors [7]. A review of the field of tactile sensors in biomedical applications revealed that although mechanoreceptors in the skin can sense strain, artificial sensors developed over the last three decades are only capable of sensing pressure [8]. A sensor that mimics biological strain sensors would be robust to the errors of occlusion that occur in optical systems and would directly measure position and velocity thus avoiding the integration drift of IMUs.

Recent work on creating wearable proprioceptive sensing systems have focused on the development and use of novel strain sensors capable of skin-like compliance. Silicone rubber with embedded microchannels of liquid metal has been used previously to measure pressure and strains [9]. The deformation in the rubber causes the microchannels to change shape and subsequently alters the electrical resistance of the embedded liquid metal "wires." By designing the structure of the rubber and microchannel paths, the sensor can be made sensitive to a specific mode of deformation such as bending [10], or to multiple modes of deformation such as two directions of strain and one of pressure [11]. Joint angle sensing of a finger joint [12] and of an ankle joint [13] have been demonstrated with the hyperelastic sensor.

Since silicone rubbers can be transparent to light, pressure sensing can be accomplished through the use of wave-guides within the rubber. Ramuz et al. [14] demonstrate an elastic device capable of sensing pressure even when stretched 70% biaxially or when wrapped around a cylinder of 3 mm radius, however they did not demonstrate curvature sensing. A recent development in stretchable strain sensors was presented by Yamada et al. [15] wherein a thin film of aligned carbon nanotubes was encapsulated in silicone rubber allowing for 300% strain and detection of leg, finger and throat motion. Similarly, Lipomi et al. [16] have demonstrated a spray-deposited film of carbon nanotubes embedded in silicone rubber that could sense strains up to 150%, but experiences significant change in its sensing range and sensitivity when strained. Spandex® yarn coated with carbon nanotubes can detect strains as large as 30% and has been used in preliminary motion sensing studies [17]. Extremely thin films of integrated electronics in soft polymers have been demonstrated as "epidermal electronics" by Kim et al. [18] and have been used as electromyographs to measure muscle activation and could withstand strains as high as 40%. Strain sensing through the use of graphite-rubber mixes have been used on tights to measure body mechanics during rowing, but have required complex calibration techniques [19]. All these previous works have demonstrated novel techniques for measuring strain, but none have demonstrated the massive strains associated with joint angle sensing integrated into a garment. In this work, we show both the performance of a highly-compliant sensor and a sensing suit that compares favorably with the gold standard of motion capture.

In Section 2 we present a description of the sensors and the sensing suit as well as the fabrication process and principles of operation. Section 3 covers the experimental methodology and results of isolated sensor characterization. The experimental methods and results of the sensor suit evaluation is found in Section 4. Finally, we discuss the conclusions of the study and topics of further study in Section 5.

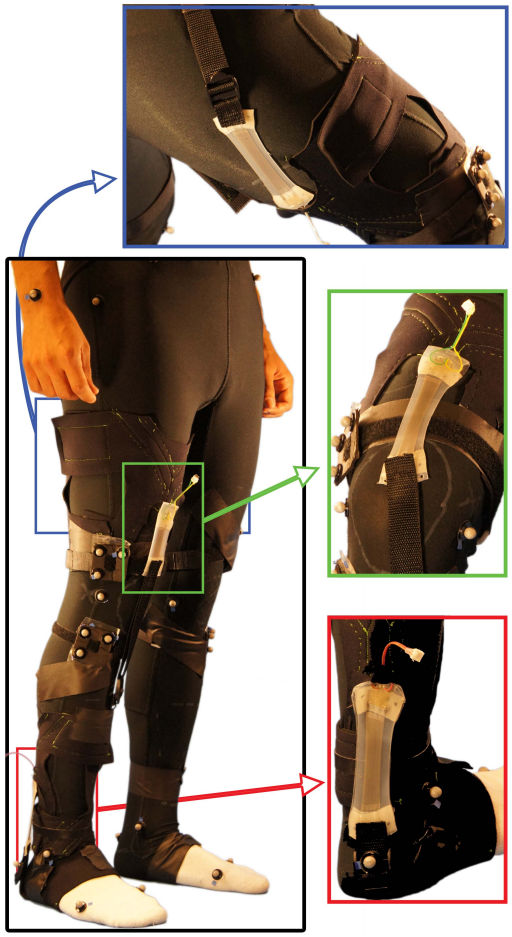

Fig. 2. A photograph of the prototype sensing suit worn by a participant. The call-outs show (from top to bottom): the hip sensor, the knee sensor and the ankle sensor.

II. System Description

We chose to use liquid metal embedded elasomer sensors because of their large strains, ease of customization by changing the sensor shape and the polymer used. The soft

sensors are based on the previous work by Majidi et al. [10], Park et al. [9] and Kramer et al. [12]. Here we present a new technology for complete body motion sensing in a simple, direct fashion with minimal computational complexity and, more importantly, in a soft wearable garment that presents minimal impedance to the motion of the wearer and is robust for outside-the-lab use. The first instantiation of this technology is presented here as soft wearable pants with integrated soft strain sensors positioned on the three major joints of the right leg (Fig. 2). The wearable system's ability to detect motion was compared with optical motion capture. Since the wearable device is constructed exclusively with soft stretchable fabrics and polymers, it interfaces exceptionally well with the body with the goal of minimizing the weight and feel of the device.

A. Hyperelastic Strain Sensor

1) Principle of Sensor Operation: The strain sensor is composed of an elastic rubber matrix with channels of liquid metal, an eutectic gallium indium (EGaIn) alloy. As this composite is strained, it lengthens in the direction of strain and contracts in the orthogonal directions according to the material's Poisson's ratio. This lengthening and contraction is applied to the channels causing an increase in the electrical resistance of the liquid metal channels due to geometric principles. These principles can be represented as:

$$\Delta R = \rho \left[\frac{L + \Delta L}{(w + \Delta w)(h + \Delta h)} - \frac{L}{wh} \right] \qquad (1)$$

where ΔR is the change in electrical resistance, ρ is the resistivity of the liquid metal, L, w and h are the length, width and height of the channels, and ΔL, Δw and Δh are the changes in length, width and height [11].

2) Sensor Fabrication: The soft strain sensor was fabricated by improving the layered molding and casting process that has been used for various types of soft sensors [9], [11], [20]. The fabrication process was divided into four major steps: silicone casting, embedding flex-circuits, bonding and injection, and final sealing. The current sensor prototype is 40 mm wide, 30 mm long and 1.5 mm thick with 0.25 mm (width and height) square cross-section embedded microchannels.

The first step, Fig. 3 (a)-(b), is to cast two separate silicone (EcoFlex0030, Smooth-On, Inc, Easton, PA 18042, USA) layers using 3D printed molds. Mesh fabrics are embedded in the bottom layer in this step. The second step, Fig. 3 (c)-(d) is to embed a flex-circuit that makes a direct contact with EGaIn microchannels between the two layers. In the third step, Fig. 3 (e)-(f), the two layers are bonded and EGaIn is injected using hypodermic needles [11]. In the final step, Fig. 3 (g)-(h), the entire sensor is sealed with the same silicone material to protect the soldered signal wires on the flex-circuit. The two major improvements in our process are the use of embedded fabric and integrated wiring.

One of the drawbacks of the previous soft sensors was the difficulty in interfacing mechanically and electrically with other materials. Due to the surface properties of silicone, chemical bonding with other materials was challenging. Moreover, direct sewing of the silicone material onto a fabric often created cracks in the silicone causing significant reduction in operating strain or lifetime. By embedding mesh fabrics at the two ends of the sensor where no mechanical strain is required, we were able to directly sew the sensor to our sensing suit without creating any notches that could lead to crack initiation.

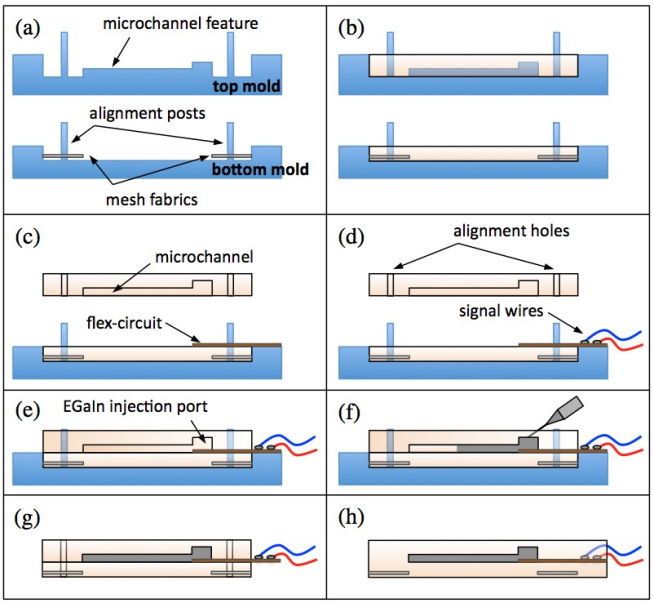

Fig. 3. Soft sensor fabrication process. (a) Prepare molds (3D printed) and mesh fabrics. (b) Pour liquid silicone. (c) Remove top mold and place flex-circuit on the bottom layer with alignment. (d) Solder signal wires on the flex-circuit. (e) Bond the top layer to the bottom layer. (f) Inject EGaIn. (g) Remove bottom mold. (h) Final sealing for wire protection.

Another difficulty in applications for soft sensors was in interfacing the highly stretchable material with traditionally inextensible electronics and wiring. Previous research on stretchable electronics has produced "wavy" silicon wiring embedded within elastomers allowing for conformal contact with skin and directly wearable electronic films [18]. However, fabrication of these embedded wires requires silicon wafer processing equipment and the handling of fragile thin-films, techniques that we avoid in our process. The design of our flexible circuit includes both copper traces and a mesh pattern of holes in the Kapton backing layer to allow for mechanical interlocking when embedded within the elastomer.

B. Sensor Suit

1) Description: The garment was designed as a single piece that could easily be worn under a layer of clothing. The base layer of the suit was a pair of elastic tights designed for running. The sensors were attached to the base layer via inextensible straps which were anchored to 2 mm thick foam neoprene that acted to stiffen the more compliant base layer. Because the sensors had fabric embedded within them, they could be attached through traditional methods such as hand or machine stitching. Each sensor also had one buckle

TABLE I

PREDICTED STRAIN OF HYPERELASTIC SENSOR ACROSS BODY JOINTS

Joint	Percentile Male Body Size 5th	50th	95th
Hip	270%	330%	380%
Knee	290%	400%	480%
Ankle	130%	140%	150%

in series with the inextensible straps to allow for manual adjustment of the sensor pre-strain which ensured the elastic sensor remained taut throughout the range of motion of the joint.

2) Joint Arc Angle Strain: The principle of joint angle sensing is based on the change in the distance between two points on the surface of body segments connected across a joint (Fig. 4). As a first order approximation, the change in length between these points can be related to the change in the joint angle and scaled by the radius of the joint, that is: $S = \theta r$. Using this equation, and applying it to anthropometry measures of joint radii and ranges of motion from the literature [21], we find that the expected strains for the sensor we present here (unstrained length of 30 mm) can reach up to 480% on the knee of a 95th percentile male (Table I).

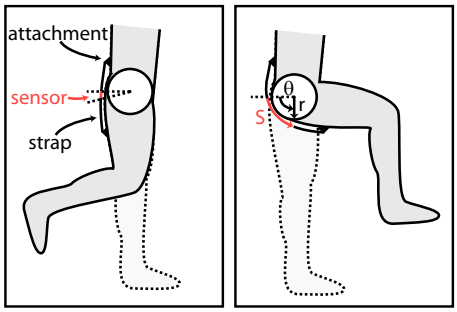

Fig. 4. The change in length between two points on the surface of the body across a joint is related to the angle and radius of the joint.

A total of three soft sensors were used (Fig. 2), spanning the ankle, knee and hip joints, respectively. The ankle joint sensor was placed posterior to the ankle joint, anchored at the base of the heel (calcaneous) and near the muscle tendon junction distal to the gastrocnemius muscle complex, stretching parallel to the Achilles tendon. The knee joint sensor was placed anteriorly to the knee joint, anchored at the head of the tibia and mid-section of the thigh. The hip sensor was placed posterior to the thigh, parallel to the biceps femoris, and anchored at the waist near the iliac crest on the distal and proximal ends.

III. SENSOR CHARACTERIZATION

A. Methods

In order to characterize the sensors separately from the sensing suit, they were sewn to inextensible straps to simulate integration to the full suit, then tested on a materials testing machine (model 5544A, Instron Inc., Norwood, MA). Extension tests were conducted on an isolated sensor. Resistance values were recorded simultaneously with force and extension values. A total of 29 extension tests were conducted on an isolated sensor to determine its physical and electrical properties. The extension rate was set to the maximum available on the tester, 25 mm/s, for every test. The total extension was set to 100, 200, 250 and 300% strain for 7 cycles each. Since the sensor has inextensible fabric embedded within the rubber, the initial length, L_0, is taken to be the extensible portion of the sensor and the strain was calculated accordingly: $\Delta L = L/30\text{mm}$. The final test was to failure.

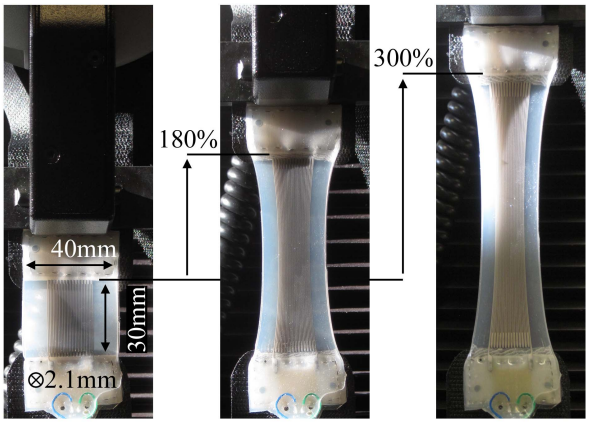

Fig. 5. Photographs of the sensor being tested in extension to characterize its mechanical and electrical properties. The sensor could reliably extend to 300% strain.

B. Results

1) Mechanical Response to Strain: The results of the isolated sensor characterization revealed that the rubber has a nonlinear elastic response and low hysteresis. In the mechanical response of the sensor (Fig. 6) there are two regions of linear stiffness. At lower extension values the rubber is fairly compliant, with a spring constant of 88.4 N/m, but after 60 mm of extension (corresponding to 200% strain) it stiffens considerably to 499 N/m. This strain-stiffening effect is more commonly seen in biopolymers than in synthetics, and is due to the constitutive polymer network strands reaching their finite maximum extensions at the molecular scale, resulting in the increase in stiffness at the macro-scale [22]. The sensor eventually fractures at an extension of 109 mm (364% strain) which required a force of 22 N. The change in the stiffness of the elastic sensor indicates that it is an important design consideration for future optimization, since it would be restricting to have a wearable sensor that suddenly stiffens at certain ranges of motion. An optimized sensor design will operate in the more compliant and relatively linear response range of the strains expected for each joint. In fact, the predicted strains at the knee of a 50th percentile male, and knee and hip of a 95th percentile male (Table I) exceed not only the low-stiffness range of the sensor's mechanical response, but also its ultimate maximum strain. Additionally, there was no change in the sensor characteristics over the number of trials, though tests of sensor lifetime and fatigue characteristics will be necessary in the future.

2) Electrical Response to Strain: Looking at the normalized signal of the sensor in response to strain (Fig. 7) one can see that the sensor has very low hysteresis and no inflection point such as those seen in the mechanical response (Fig. 6). The lack of significant inflection points is because the sensor response is directly related to geometric effects, and so is insensitive to the stiffness of the material. The inset shows the difference in the loading and unloading paths of the sensor signal. A linear fit approximates the sensor response very well (R^2=0.9924), and is convenient for later comparison and calibration requirements. In our analysis we make a naive assumption on the linearity of sensor response in strain in order to examine the relationship of strain to joint angle. Though joint motion is complex, we assume that the sensor motion across the joint is linear in order to compare sensor response in isolation directly with sensor response when worn on the body. As expected, the sensor signal goes to infinity at failure due to the fracture of the conductive channels.

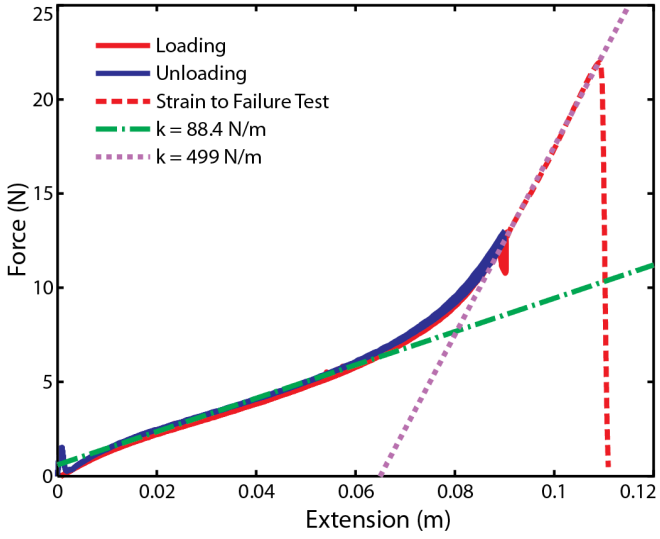

Fig. 6. The results of seven repeated extension tests and one failure test for a single representative sensor. The extension rates in both loading and unloading were 25 mm/s. The dashed lines are fitted to the linear regions to indicate the change in stiffness as the rubber sensor is strained. The sensor failed at an extension of 109 mm (364% strain).

IV. Sensor Suit Evaluation

A. Methods

Kinematic data was collected at the Wyss Institutes's Motion Capture Laboratory. Procedures were approved by the Harvard Medical School Committee on Human Studies. One healthy male participant took part in this study after written consent.

Motion capture data collection was based on established body marker placements and calibration techniques [23], [24]. A Vicon® motion analysis system with eight infrared cameras (Oxford Metrics, Oxford, UK) was used. A total of 44 markers were attached to the participant based on a

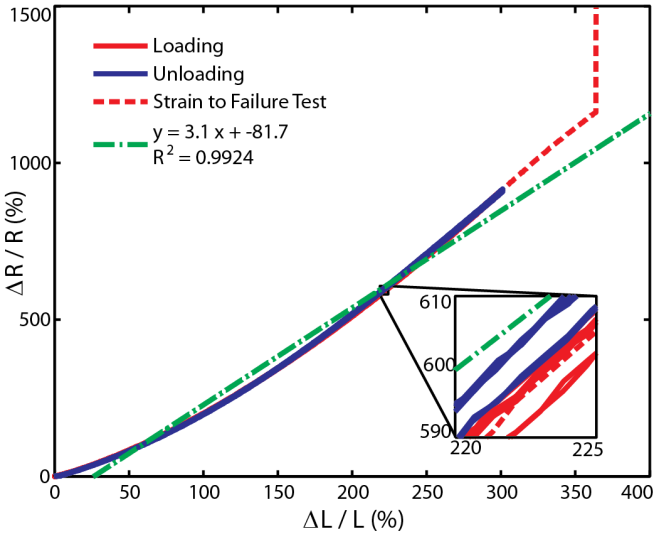

Fig. 7. The normalized sensor signal is highly repeatable and has very low hysteresis. When the sensor fractures, the resistance goes to infinity, as can be seen in the dashed red line of the failure test. The inset shows the tight packing of the paths of the sensor signals. A linear fit to the cyclic portion of the signal shows a gain (slope) of 3.1 %/%.

modified Cleveland Clinic marker set. Lower body markers were placed on the following anatomical landmarks: bilateral anterior superior iliac spines, bilateral apex of the iliac crests, dorsal aspect at the L5-sacral interface, lateral and medial femoral condyles, lateral and medial malleoli, calcaneal tuberosities and the superior aspect of the first and fifth metatarsophalangeal joints. Triad marker clusters were placed on the femora and tibiae. Upper body markers were placed at the forehead, left and right temple, seventh cervical vertebra, sternum, tip of the tip of the acromia processes, humeral lateral epicondyles and the midpoint between the radial and ulna styloid processes. Motion capture data was collected at a sampling rate of 120 Hz. OpenSim 3.0 was used to scale a 23 degrees of freedom head, torso and lower limb model to the participant based on 14 anthropomorphic measurements. After scaling the generic model, an inverse kinematic analysis was performed which calculated anatomical joint angles given the three dimensional marker trajectories [2].

Sensor data from the sensor suit was collected simultaneously with the motion capture data using a custom electronics board based on an ATMEL AVR Mega1280 microcontroller development board with eight analog inputs, each of which provide 10 bits of resolution, at a sampling rate of 50 Hz. Motion capture and sensor suit data was synchronized and analyzed using custom MATLAB® code.

To evaluate the sensing suit, we focused on two tasks: range of motion and gait. Dynamic range of motion evaluations were performed while standing. The participant was asked to flex and extend his dominant leg's ankle, knee, and hip joint individually (sagittal plane motions) reaching the comfortable limits of each joint's range of motion (Fig. 8). The participant performed five trials of each joint motion, for durations of 20 seconds each. For the gait evaluation, the

participant was asked to walk at a self-selected walking speed along a 5.5 m walk-way for 10 consecutive trials (Fig. 9). The participant took six strides in the space of the walk-way before stopping, so the first two and last two full strides where transient behavior generally occurs were ignored, and the analysis focused entirely on the two full strides in the middle of each trial.

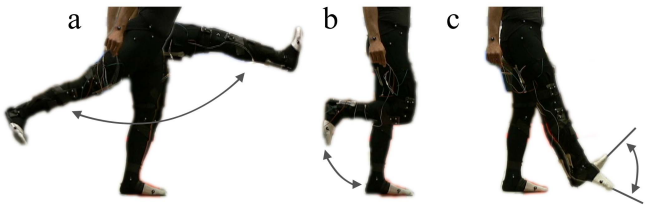

Fig. 8. To determine sensor response on the body, the participant was asked to sweep out the range of motion for each of the instrumented joints: (a) hip, (b) knee and (c) ankle.

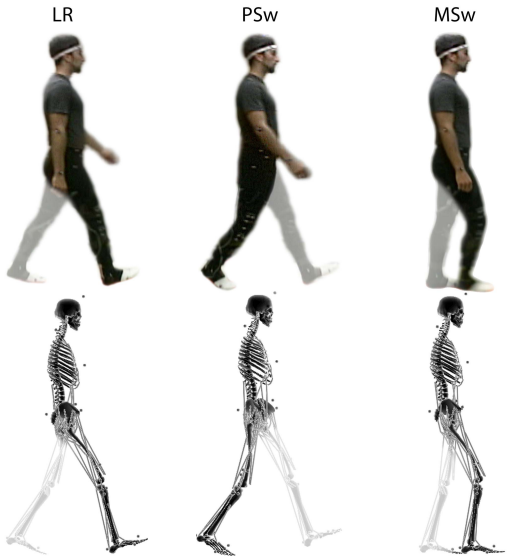

Fig. 9. The walking trial had the participant walk at a self-selected speed along a straight path through the motion capture work-space. The top row of images are video stills and the bottom row are the corresponding Vicon motion capture poses visualized in OpenSim.

All data from the Vicon motion capture system and the sensing suit were recorded separately, so the data was first synchronized with a manually applied time offset for each pair of data from a given trial. No filtering was applied to either the Vicon or sensing suit data. Next, in order to make direct comparisons between the sets of data, the Vicon data was downsampled from 120 Hz to 100 Hz and the sensing suit data was upsampled from 50 Hz to 100 Hz. The sampling was done with MATLAB's spline interpolating function, a third order function. Finally, to compare the sensing suit data directly to Vicon, in each pair of data samples the sensing suit voltage signal were fitted to the Vicon joint angle signal with a first order polynomial fit.

B. Results

1) Dynamic Range of Motion: The data from the sensing suit was compared directly with the joint angles provided by the OpenSim model based analysis of the Vicon optical motion capture data. The sensor response during the dynamic range of motion tests of the joints showed greater variation and significant hysteresis in comparison to standing trials. Both the increased variation and hysteresis can be attributed to the interface of the sensors to the body. Linear fitting was for simplicity and shows that even without complex algorithmic fitting, the sensing suit can accurately track joint angle. The best coefficient of determination (R^2 value) of 0.9680 was found at the ankle sensor (Fig. 10c), followed by 0.9646 at the hip (Fig. 10a), then 0.9436 at the knee sensor (Fig. 10b). It is important to note that the limits of motion seen in the data are on account of the limits of the participant, not the sensor. Although the suit is designed to be adjustable, with buckles in series with the sensors used to apply a desired amount of pre-strain, it was qualitatively observed that the sensor response would vary if the suit was shifted during testing. This systematic variability can be accounted for in future versions with redundant sensor placement, better tailoring of the suit, and appropriate algorithms.

2) Gait Trials: To analyze the gait trials, the sensor suit and Vicon data were fitted to a percentage of the gait cycle (Fig. 11). The sensor suit signals were fitted to the their respective joint angles using a linear least squares fitting method, as was done when evaluating the isolated sensor in extension (Fig. 7) and during dynamic range of motion trials (Fig. 10). Qualitatively, the sensor suit is effective at tracking the joint angles and giving a good sense of the participant's gait cycle state. The hip sensor has an especially close fit to the Vicon ground truth throughout the gait cycle. The knee has a good fit in terms of phase and accurately reflects the knee angle during swing phase (30% to 90% gait cycle) but underestimates the knee angle during the stance phase (0% to 20%). The ankle sensor signal tracks the joint angle least precisely, displaying an apparent phase shift as well as variable gain.

Quantitatively, all three sensors tracked the joint angles with mean absolute errors (MAE) of less than 8° at any given instance during the gait cycle. The hip sensor was the most precise in tracking, and showed a peak MAE of only 5°. The linear fits for the sensor signals were calculated separately for each joint and for each trial, and the fit had the form: $y = mx+b$, where y was the sensor signal in percent change in resistance ($\%(\Delta R/R)$), x was the joint angle in degrees (°), b was the signal offset in percent change in resistance ($\%(\Delta R/R)$), and m was the gain in degrees over percent change in resistance ($^\circ/[\%(\Delta R/R)]$). The fitting parameters can be found in Table II and can be directly compared to the values in Figure 10. The gain of the linear fitting for the sensor signals was significantly different from the dynamic range of motion trials. The hip gain changed the least; it was 8.35 (%/○) during walking as compared to 9.08 (%/○) during standing trials. The knee gain was 8.63 (%/○) for walking

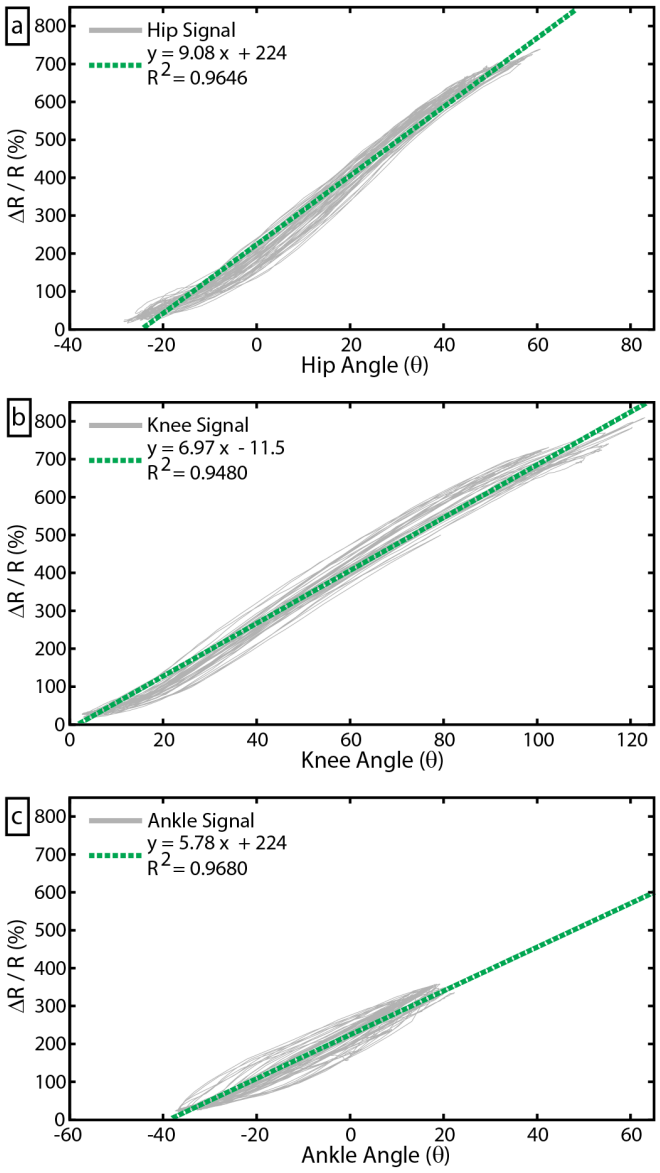

Fig. 10. The sensor response to standing dynamic range of motion trials for (a) hip, (b) knee, and (c) ankle (for each graph, N = 5 trials, 1 participant). The signal shows some hysteresis from loading to unloading, but a linear approximation fit the data well.

and 6.97 (%/○) for standing and the ankle was 6.42 (%/○) during walking and 5.78 (%/○) during standing.

The change in gains from standing to walking trials and the phase shifts observed in the sensors during walking can be related to the hysteresis and nonlinearity observed in the sensor response during dynamic range of motion trials (Fig. 10). Since the sensors themselves show almost no hysteretic response during isolated extension tests (Fig. 7), we hypothesize that the hysteresis is entirely due to the manner in which the sensors were integrated to the body, i.e. the suit itself. Sources for error can include any slipping between the elastic base layer and the skin and loosening of the sensor attachments. Future work will investigate the use of reversible adhesives that may reduce slipping on skin

TABLE II

WALKING LINEAR FITTING PARAMETERS

Joint	m	b	R^2
Hip	8.35	223	.9997
Knee	8.63	-45.1	.9922
Ankle	6.42	193	.9740

as well as redundancy in sensor integration to capture joint information even when the suit shifts on the body.

V. CONCLUSIONS

In this report we have presented a wearable sensing suit for lower extremity biomechanics that uses hyperelastic strain sensors positioned to measure joint angles via applied strains. Such a soft sensing suit could provide a useful tool for physical therapy tasks. For example, joint range of motion could be recorded and tracked over multiple therapy sessions or signals from the sensors could be interfaced to a game or virtual environment to provide an engaging experience for the patient. The technology in this sensor suit will also be applicable to the intelligent and low profile wearable systems developed in DARPA's Warrior Web program (BAA-11-72); the sensor signals will be used to inform the control of actuators to provide joint assistance at the appropriate time or to monitor soldier activity and performance in the field.

In future work, improved attachment of sensors to the base layer will reduce hysteresis and improve angle tracking. We plan to optimize sensor dimensions for respective joints to improve sensitivity and robustness. These sensor improvements will be accompanied by kinematics studies to quantitatively identify the degree of impact the suit has on the wearer. Future work will also emphasize both redundant sensor placement as well as improved positioning to increase robustness to garment shifting. Finally, we will fully instrument all lower extremity degrees of freedom in order to capture not only sagittal-plane motions, but also motions in the coronal and mediolateral planes. This full instrumentation and the development of a sensor initialization/calibration procedures independent of Vicon will realize our goal of an outside-the-lab motion capture device.

REFERENCES

[1] M. Wehner, Y.-L. Park, C. J. Walsh, R. Nagpal, R. J. Wood, T. Moore, and E. Goldfield, "Experimental characterization of components for active soft orthotics," *International Conference on Biomedical Robotics and Biomechatronics (BioRob)*, pp. 1586–1592, June 2012.

[2] S. L. Delp, F. C. Anderson, A. S. Arnold, P. Loan, A. Habib, C. T. John, E. Guendelman, and D. G. Thelen, "OpenSim: open-source software to create and analyze dynamic simulations of movement.," *IEEE Transactions on Bio-Medical Engineering*, vol. 54, pp. 1940–50, Nov. 2007.

[3] K. Yoshino, T. Motoshige, T. Araki, and K. Matsuoka, "Effect of prolonged free-walking fatigue on gait and physiological rhythm.," *Journal of biomechanics*, vol. 37, pp. 1271–80, Aug. 2004.

[4] S. Patel, H. Park, P. Bonato, L. Chan, and M. Rodgers, "A review of wearable sensors and systems with application in rehabilitation.," *Journal of Neuroengineering and Rehabilitation*, vol. 9, p. 21, Jan. 2012.

[5] O. J. Woodman, "An introduction to inertial navigation," *Technical Report UCAM-CL-TR-696*, 2007.

[6] D. De Rossi and P. Veltink, "Wearable technology for biomechanics: e-textile or micromechanical sensors?," *IEEE Engineering in Medicine and Biology Magazine*, vol. 29, no. 3, pp. 37–43, 2010.

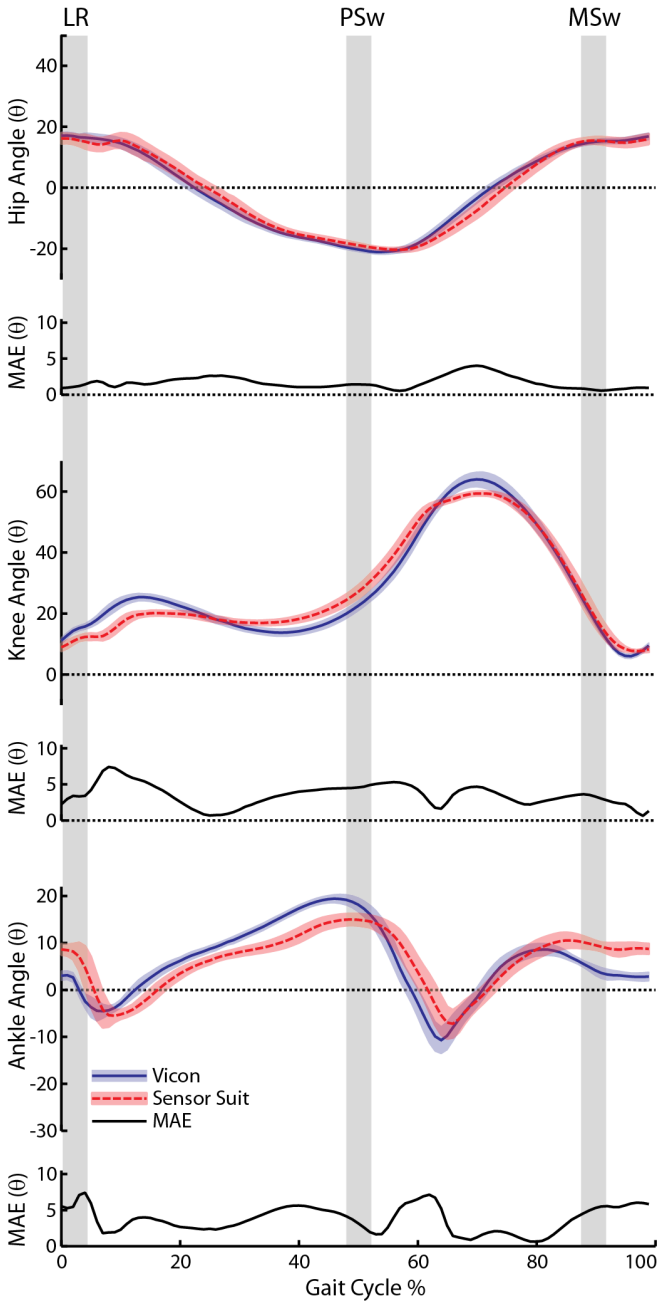

Fig. 11. The means and standard deviations (shaded region) of joint angles determined by the Vicon system and the sensor suit and the mean absolute error (MAE) are plotted against the gait cycle percentage (N = 10 gait trials, 1 participant). The vertical bars represent regions of the gait cycle corresponding to three still frames in Figure 9 (from left to right): Loading Response (LR), Pre-Swing (PSw), and Mid-Swing (MSw).

[7] E. Kandel, J. Schwartz, and T. Jessell, *Principles of Neural Science*. McGraw-Hill Medical, 2000.

[8] M. I. Tiwana, S. J. Redmond, and N. H. Lovell, "A review of tactile sensing technologies with applications in biomedical engineering," *Sensors and Actuators A: Physical*, vol. 179, pp. 17–31, June 2012.

[9] Y.-L. Park, C. Majidi, R. K. Kramer, P. Bérard, and R. J. Wood, "Hyperelastic pressure sensing with a liquid-embedded elastomer," *Journal of Micromechanics and Microengineering*, vol. 20, p. 125029, Dec. 2010.

[10] C. Majidi, R. K. Kramer, and R. J. Wood, "A non-differential elastomer curvature sensor for softer-than-skin electronics," *Smart Materials and Structures*, vol. 20, p. 105017, Oct. 2011.

[11] Y.-L. Park, B.-r. Chen, and R. J. Wood, "Design and Fabrication of Soft Artificial Skin Using Embedded Microchannels and Liquid Conductors," *IEEE Sensors Journal*, vol. 12, pp. 2711–2718, Aug. 2012.

[12] R. K. Kramer, C. Majidi, R. Sahai, and R. J. Wood, "Soft curvature sensors for joint angle proprioception," in *2011 IEEE/RSJ International Conference on Intelligent Robots and Systems*, pp. 1919–1926, IEEE, Sept. 2011.

[13] Y.-L. Park, B.-r. Chen, D. Young, L. Stirling, R. J. Wood, E. Goldfield, and R. Nagpal, "Bio-inspired active soft orthotic device for ankle foot pathologies," *2011 IEEE/RSJ International Conference on Intelligent Robots and Systems*, pp. 4488–4495, Sept. 2011.

[14] M. Ramuz, B. C.-K. Tee, J. B.-H. Tok, and Z. Bao, "Transparent, optical, pressure-sensitive artificial skin for large-area stretchable electronics.," *Advanced Materials*, vol. 24, pp. 3223–7, June 2012.

[15] T. Yamada, Y. Hayamizu, Y. Yamamoto, Y. Yomogida, A. Izadi-Najafabadi, D. N. Futaba, and K. Hata, "A stretchable carbon nanotube strain sensor for human-motion detection.," *Nature Nanotechnology*, vol. 6, pp. 296–301, May 2011.

[16] D. J. Lipomi, M. Vosgueritchian, B. C.-K. Tee, S. L. Hellstrom, J. A. Lee, C. H. Fox, and Z. Bao, "Skin-like pressure and strain sensors based on transparent elastic films of carbon nanotubes.," *Nature Nanotechnology*, vol. 6, pp. 788–92, Jan. 2011.

[17] R. Zhang, H. Deng, R. Valenca, J. Jin, Q. Fu, E. Bilotti, and T. Peijs, "Carbon nanotube polymer coatings for textile yarns with good strain sensing capability," *Sensors and Actuators A: Physical*, vol. 179, pp. 83–91, June 2012.

[18] D.-H. Kim, N. Lu, R. Ma, Y.-S. Kim, R.-H. Kim, S. Wang, J. Wu, S. M. Won, H. Tao, A. Islam, K. J. Yu, T.-i. Kim, R. Chowdhury, M. Ying, L. Xu, M. Li, H.-J. Chung, H. Keum, M. McCormick, P. Liu, Y.-W. Zhang, F. G. Omenetto, Y. Huang, T. Coleman, and J. A. Rogers, "Epidermal electronics.," *Science*, vol. 333, pp. 838–43, Aug. 2011.

[19] M. Tesconi, A. Tognetti, E. P. Scilingo, G. Zupone, N. Carbonaro, D. De Rossi, E. Castellini, and M. Marella, "Wearable sensorized system for analyzing the lower limb movement during rowing activity," *2007 IEEE International Symposium on Industrial Electronics*, pp. 2793–2796, June 2007.

[20] D. Vogt, Y.-L. Park, and R. J. Wood, "Multi-Axis Force Sensing in a Soft Artificial Skin," in *to appear in Proceedings of IEEE Sensors 2012 Conference*.

[21] Henry Dreyfuss Associates, *The Measure of Man and Woman: Revised Edition*. New York: John Wiley & Sons, 2002.

[22] K. A. Erk, K. J. Henderson, and K. R. Shull, "Strain stiffening in synthetic and biopolymer networks," *Biomacromolecules*, vol. 11, pp. 1358–63, May 2010.

[23] M. P. Kadaba, H. K. Ramakrishnan, and M. E. Wootten, "Measurement of lower extremity kinematics during level walking.," *Journal of Orthopaedic Research*, vol. 8, pp. 383–92, May 1990.

[24] D. A. Winter, *Biomechanics and Motor Control of Human Movement*. New York: John Wiley & Sons, 1990.